



## Research article

# Quality-by-design based fabrication of febuxostat-loaded nanoemulsion: Statistical optimization, characterizations, permeability, and bioavailability studies

Vishal C. Gurumukhi<sup>a</sup>, Vivek P. Sonawane<sup>b</sup>, Ganesh G. Tapadiya<sup>a</sup>, Sanjaykumar B. Bari<sup>c</sup>, Sanjay J. Surana<sup>d</sup>, Shailesh S. Chalikwar<sup>d,\*</sup><sup>a</sup> Department of Pharmaceutical Quality Assurance, Shreeyash Institute of Pharmaceutical Education and Research, Aurangabad 431010, Maharashtra, India<sup>b</sup> Department of IPQA, Micro Labs Ltd, Verna Industrial Estate, Goa 403722, India<sup>c</sup> Department of Pharmaceutical Chemistry, H. R. Patel Institute of Pharmaceutical Education and Research, Shirpur 425 405, Maharashtra, India<sup>d</sup> Department of Industrial Pharmacy and Pharmaceutical Quality Assurance, R. C. Patel Institute of Pharmaceutical Education and Research, Shirpur 425 405, Maharashtra, India

## ARTICLE INFO

## Keywords:

Quality by design  
Febuxostat  
Box behnken design  
Bioavailability

## ABSTRACT

The present work deals with QbD-based development of FEB-loaded nanoemulsion (FEB-NE) in order to enhance bioavailability and permeability. In the beginning, the risk assessment was performed on different experimental variables using the Ishikawa diagram followed by FMEA study in order to find critical process parameter (CPP) and critical material attributes (CMAs). To build quality in nanoemulsion, the quality target product profiles (QTPP) and critical quality attributes (CQAs) were determined. The different batches of FEB-NE were produced by the microemulsification-probe sonication method. Effect of varying levels of independent variables such as oil concentration ( $X_1$ ),  $S_{mix}$  concentration ( $X_2$ ), and amplitude ( $X_3$ ) on responses such as globule size ( $Y_1$ ), zeta potential ( $Y_2$ ), and entrapment efficiency ( $Y_3$ ) were studied using Box-Behnken design (BDD). FEB-NE formulation was optimized using a graphical and numerical method. The optimized formulation concentrations and their responses (CQAs) were located as design space in an overlay plot. The spherical shapes of globules were visualized by surface morphology using AFM and TEM. *In vitro* dissolution study showed 93.32% drug release from the optimized FEB-NE formulation. The drug release mechanism followed by the formulation was the Higuchi-matrix kinetics with a regression coefficient of 0.9236 ( $R^2$ ). FEB-NE showed enhanced permeability using PAMPA (artificial non-cell membrane) and everted gut sac model method. The developed optimized FEB-NE exhibited the enhancement of bioavailability by 2.48 fold as compared to FEB-suspension using Wistar rats suggesting improvement of solubility of a lipophilic drug. The optimized batch remained stable for 90 days at 4 °C and 25 °C. Thus, QbD-based development of FEB-NE can be useful for a better perspective on a commercial scale.

\* Corresponding author. Department of Industrial Pharmacy and Quality Assurance, R. C. Patel Institute of Pharmaceutical Education and Research, Shirpur 425 405, Maharashtra, India.

E-mail addresses: [sschalikwar@rcpatelpharmacy.co.in](mailto:sschalikwar@rcpatelpharmacy.co.in), [pharmashailsh@rediffmail.com](mailto:pharmashailsh@rediffmail.com) (S.S. Chalikwar).

<https://doi.org/10.1016/j.heliyon.2023.e15404>

Received 29 November 2022; Received in revised form 24 March 2023; Accepted 6 April 2023

Available online 18 April 2023

2405-8440/© 2023 Published by Elsevier Ltd.

This is an open access article under the CC BY-NC-ND license

(<http://creativecommons.org/licenses/by-nc-nd/4.0/>).

## 1. Introduction

Febuxostat (FEB) is a potent and novel orally administered non-purine selective xanthine oxidase inhibitor used for the treatment of gout [1]. It works as a xanthine oxidase inhibitor for its oxidized and reduced forms [2]. It is recommended typically to reduce the urate level in patients suffering from gout [3]. Gout is produced by a condition known as hyperuricemia, where an excessive deposition of uric acid in joints by which the patient experiences tremendous pressure and pain. Hyperuricemia is a risk factor for patient who has serum urate levels of more than 6.8 mg/dL due to the production of monosodium urate crystals (MSU) [4].

To manage such a painful form of arthritis, FEB is a drug of choice for chronic gout conditions approved by the FDA (United States Food and Drug Administration). FEB is a weak acid (pKa value 3.08) and falls under the category of class II having limited solubility and high permeability [5]. The oral bioavailability is hindered due to the first-pass effect and the concentration of drug is decreased by 38–39% in presence of food which results in reduced clinical applications [3].

Hence, there is a strong need to develop a new approach with novel formulation development for the treatment of gout. Several formulations containing FEB exist in the market for oral administration. In that, self-microemulsion [6], liposomes [7], and nanoemulsion [8]. A literature survey showed several reports on nanocrystals [9], neosomal gel [3], and nanosuspension [5]. However, these formulations have their limitations like low entrapment efficiency, leakage issues, and lack of stability [10]. Apart from these, scale-up difficulty, high manufacturing cost, and storage stability are the issues of liposomes [11]. Moreover, the sedimentation and compaction problems of suspension [12] and reduced shelf life, aggregation, drug leakage, instability, and a fusion of vesicles of neosomal gel [10,13] are the several issues that limit its clinical applications.

Among these strategies, the nanoemulsion (NE) formulation has emerged recently as a versatile and emerging choice that provides steric stabilization potential between droplets, ease of absorption, increased solubility, permeability of drugs, and targeted delivery of drug [14,15]. The selection of excipients is equally important for the development of NE that can provide the platform for various insoluble drugs which results in higher drug loading and improve stability issues for commercial potential [10].

Despite the advantages, there are still certain legal issues and unanswered questions regarding the development of nanoformulations. Numerous attempt has been made for the optimization process of NE involving one variable at a time (OVAT) while keeping other variable constants in which interactions of variables and their effect is not possible [16,17]. The development of products is traditionally by quality by testing (QbT) technique which is outdated and has no guarantee of quality for the developed product [18]. Many government bodies such as USFDA, EMEA, and MHRA do not encourage QbT. It is very commendable to use a quality-by-design (QbD)-based strategy in novel formulation development [19].

QbD is extremely recommended for building predefined quality in product with assurance and understanding at a higher level. Time and cost saving is one of the benefits during development of a product using QbD. International Council for Harmonisation (ICH) guidelines such as Q8: Pharmaceutical Development, Q9: Quality Risk Management, and Q10: Pharmaceutical Quality System highlighted requirements and necessary implementation of regulatory bodies like FDA and EMA [20].

In the present paper, we prepared FEB-loaded NE by microemulsification-probe sonication method using QbD based approach concerning the context of the predecided quality target product profile (QTPP). Secondly, elements of QbD framework such as critical process parameters (CPPs) and critical quality attributes (CQAs) have been identified whose variability affects the QTPP [21]. For the development of NE, the experimental variables were isolated by risk assessment techniques which results in the prediction of parameters that affects the product quality. Several experimental runs and optimized FEB-NE formulation were performed using Box-Behnken Design (BBD). The morphology of globules was studied by atomic force microscopy (AFM), and transmission electron microscopy (TEM). Drug release was monitored using dissolution studies. Permeability of FEB was observed using non-cell artificial membrane method and gut sac model method. The *in vivo* studies using Wistar rats were conducted for improved bioavailability.

## 2. Materials and methods

### 2.1. Materials

FEB (Purity >99.0%) was kindly gifted by Lupin Research Park Pvt. Ltd. (Aurangabad, India). Various oils such as Captex 355P, Captex 200P, Captex 355P, Capmul MCM, Capmul PG-12, and Capmul MCM were donated by Abitec Corporation Ltd. (Germany). Labrafil, Lauroglycol™ 90, Transcutol HP, Labrasol, and Capryol 90 were obtained as a gift from Gattefosse Pvt. Ltd. (USA). Sunflower oil, Oleic acid, Cotton seed oil, and Olive oil were purchased from the local market. Various surfactants such as Tween 80, Tween 20, Span 80, PEG 200, and PEG 400 were obtained from Jinendra Scientific Pvt. Ltd. (Jalgaon, India). Lipoid E80 was gifted by Lipoid GmbH (Germany). Methanol (Pure) and Ethanol (Pure) were obtained from Merck (India). Dimethyl Formamide (DMF) and Dimethyl Sulfoxide (DMSO) were bought from Jinendra Scientific Pvt. Ltd. (Jalgaon, India). Double distilled water (DDW) was prepared in the laboratory. The remaining chemicals and required reagents of analytical grade were procured and used in our experiment without re-purification.

### 2.2. Animals

Wistar rats (male) around weight 175–185 g were allotted and housed in a cage with the provision of light and air in the laboratory of R. C. Patel Institute of Pharmaceutical Education and Research (An Autonomous Institute) Shirpur, Dhule. Animals were kept to acclimatize for 7 days before the study and provided with free water, feed, light, and air.

## 2.3. Methods

### 2.3.1. HPLC analysis

The amount of FEB was established with slight modification by RP-HPLC method using the earlier reported method [1]. Briefly, chromatography was performed using column, princetonSHER Ultima C-18 as a stationary phase with a dimension of (250 mm × 4.6 mm × 5 μm). The mobile phase consisting of Methanol: Potassium Dihydrogen Phosphate 10 mM Buffer, pH: 6.8 (70:30) was pumped with a flow rate of 1.2 mL/min. The sample of volume 20 μL was injected into the HPLC system and detected by Waters 2996 Photodiode Array Detector (PDA) at 315 nm. The calibration curve was constructed using a linearity range 10–50 μg/mL and obtained the regression coefficient ( $r^2 = 0.999$ ). The estimated and developed method was validated in accordance with guidelines rendered by ICH Q2 (R1) (2005) [22].

### 2.3.2. Choice of oil

For development of NE, the screening of oils and surfactants was performed. The described previously shaking flask process was used for the assessment of solubility of FEB in various oils and surfactants [23]. The oil sample (1.0 mL) mixing with an excess quantity of FEB was mixed with the aid of cyclomixer at a room temperature for a period of 48 h (Remi CM-101).

The oils used for screening such as Capmul PG 12, Captex 355P, Captex 200P, Cottonseed oil, Sunflower oil, Olive oil, Capmul MCM, Labrafil, Oleic acid, Peceol, and Lauroglycol 90 respectively. Equilibrated samples were centrifuged and the supernatant was isolated.

Further, the supernatant was filtered employing a 0.45 μm membrane filter. It was diluted suitably with methanol and amount of FEB was analyzed using absorbance at 315 nm on UV-visible spectrophotometer [24]. Each study was accomplished in triplicate.

### 2.3.3. Choice of surfactant

The appropriate surfactant was screened based on the highest solubility of FEB in the surfactant [25]. The surfactants such as Tween 80, Tween 20, PEG 200, PEG 400 Transcutol HP, Labrasol and Capryol 90, and Lipoid E80 were screened for solubility of FEB. In brief, an excess quantity of FEB was added to a test tube containing a fixed amount (1 mL) of surfactant and mixed for 5 min with a vortex mixture (Vortex-GeNei 2). Further, this sample was centrifuged at 4000 rpm for 10 min. The separated supernatant was diluted suitably using methanol and absorbance was taken at 315 nm. Thus, the dissolved amount of FEB was determined in triplicate using a calibration curve constructed previously [26]. Further, co-surfactant (as a secondary surfactant) was selected based on solubility and HLB values. Thus, surfactant and co-surfactant and their ratio were decided based on particle size, stability, and HLB value [27].

### 2.3.4. Pseudoternary phase diagram to optimize the NE components

In order to construct pseudo-ternary phase diagram, the screened components such as oil, surfactant, and co-surfactant were utilized in the spontaneous emulsification method [28]. Initially, the different ratios of surfactant and co-surfactant (1:1, 2:1, 3:1, 4:1% w/v) were selected to prepare  $S_{mix}$  at room temperature. Afterward, selected oil and specific  $S_{mix}$  in varying ratios 1:9 to 9:1% w/v to mark out the phase boundaries were mixed. The resulting solution was titrated against double-distilled water with stirring to obtain an equilibrium phase. The solution was observed for clear, translucent, and single-phase NE. This NE was kept for 12 h under observation for phase separation and after confirmation of the unseparated NE, a ternary phase diagram was constructed using CEMEX school software [15,29].

## 2.4. QbD-based nutshell

### 2.4.1. Assignment of QTPP for NE

In QbD based nutshell, the development of NE was initiated by assigning QTPP with a view of a patient-centric approach [16]. Several factors in association with QTPP and their justifications are summarized in Table 1. The experimental attributes (CQA) such as globule size, zeta potential (ZP), and entrapment efficiency (EE) are the responses for the experimental variables. Table S1 (provided as supplementary) summarized the experimental attributes (CQA) and their justifications.

**Table 1**  
QTPP elements for production of nanoemulsion with their justification.

| QTPP                    | Target   | Justification(s)  |
|-------------------------|--|---|
| Dosage form             | Nanoemulsion   | Liquid dosage form is a preferred choice of adults and childrens  |
| Dosage Type             | Controlled release   | Superior absorption potential possible with controlled release  |
| Route of administration | Oral   | Most preferred route for all includes adults and childrens for the treatment of Gout  |
| Drug content            | 85–95%   | To maintain therapeutic requirement and need of treatment   |
| Drug release            | More than 85%  | Required for effective therapy and improve bioavailability of drug  |
| Pharmacokinetics        | Maximum $C_{max}$ , $T_{max}$ and AUC determines performance | The maximum plasma concentration attained vurses time provides higher drug absorption rate and extent including evaluation of efficacy and safty data |
| Stability               | 12 months  | The therapeutic potential of the drug in nanoemulsion stabilies during storage period   |

#### 2.4.2. Risk assessment studies

Experimental factors involved in the development of NE were identified by plotting the Ishikawa diagram (Fig. 1). The factors which possess risk and have an effect on responses were studied using FMEA based on RPN score. All these elements are based on scientific knowledge, literature, and past experience [30]. The RPN score formula was determined using the product of severity (S), occurrence (O), and detection (D).

Thus, based on RPN score, the identified experimental variables i.e. CPPs and CMAs were employed with three different levels (i.e. low, medium, and high) to investigate the influence on critical attributes using BBD method.

#### 2.4.3. Preparation of optimized placebo NE

After several trials, a transparent NE was obtained from a pseudo-ternary phase diagram. This batch was used as an optimized batch and considered to be a placebo formulation for further study. Various primary parameters of the placebo batch were examined which include, heating-cooling cycle, freeze-thaw test, and centrifugation test of NE [26]. The creaming, phase separation, and opalescence of NE were observed visually. The optimization of the formulation was done based on the desired clarity, globule size, ZP, and EE.

#### 2.4.4. Heating cooling cycle and centrifugation test

For the heating and cooling cycle, the placebo formulation was placed at 4 °C (refrigerator temperature) to 45 °C (high temperature) for at least not less than 48 h. Each formulation was subjected to six cycles in order to determine the results.

Phase separation was conducted by centrifugation method in which each formulation was centrifuged at 2000 rpm for 15 min using an ultracentrifuge (Beckman colter Optima max-XP) [31]. A qualifying formulation was used for further studies.

#### 2.4.5. Freeze-thaw test

The stability of NE was further observed in various conditions using Freeze-thaw cycle. The rapid and sudden temperature change applied to the test sample of NE can experience in several shipping process [32].

#### 2.4.6. Production of FEB loaded nanoemulsion (FEB-NE)

The components were selected for the preparation of NE based on preformulation studies such as solubility test and pseudo-ternary phase diagram. The nanoemulsion (NE) containing FEB was formulated by the microemulsification-probe sonication method [27]. Schematic representation for the production of NE are shown in Fig. S1. Briefly, a measured amount of Captex 200P and  $S_{mix}$  (2:1) was mixed using a magnetic stirrer (Remi 2 MLH) with 700 rpm and maintaining a temperature above 45 °C. To this phase, the required amount of FEB was incorporated. On the other hand, the water phase maintained the same temperature as that of oil phase. Here, the order of mixing of excipients was significant in the preparation of NE.

The aqueous phase was added dropwise into the oil phase using a syringe while stirring to form a microemulsion. Further, this preparation was homogenized using Ultra Turrax (IKA-T23) at 11,000 rpm for 9 min at 50–60 °C. The sample was then applied to ultrasonication using a probe sonicator (PCI Analytics Pvt. Ltd., Mumbai, India) with optimized 40% amplitude to obtain NE. The hot NE was subsequently kept aside at room temperature for further study.

#### 2.4.7. Box-Behnken Design (BDD)

The influence of various experimental variables was investigated using BDD of the experiment. For the development of FEB-NE and

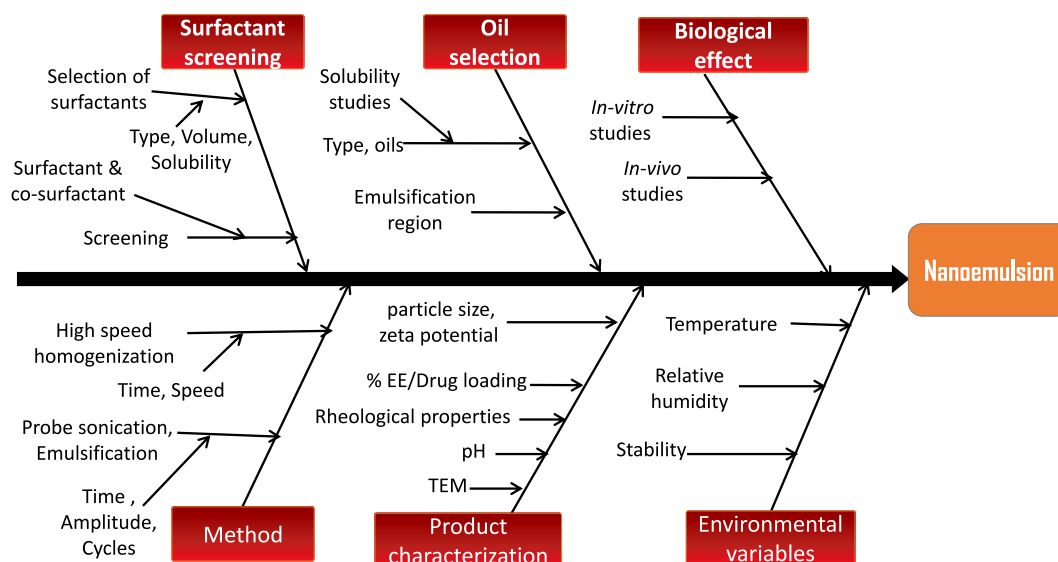


Fig. 1. Ishikawa diagram showing relationship between CPP and CMA for the preparation of NE.

its optimization BDD with three factors, three levels were chosen. This is the best experimental model for response surface methodology. Because it allows to facilitate evaluation of the quadratic model parameters and the construction of subsequent designs. The lack of fit of the model recognition and appropriate use of blocks can be possible. Moreover, using this design, experimentation under extreme conditions can be avoided so as to obtain satisfactory results. In addition, in BDD design allows fewer experimental runs where the number of factors is three [32].

The experimental variables were selected based on the screening methodology for employment in the design of experiments (DoE). The oil ( $X_1$ %) and  $S_{mix}$  ( $X_2$ %) and amplitude ( $X_3$ %) were selected as the experimental variables with three coded levels (-1, 0, +1) which have an impact on responses such as globule size ( $Y_1$ ), ZP ( $Y_2$ ) and EE ( $Y_3$ ). In this design, 17 experiments were run of which 5 experiments were replicated (Table 2). Data were analyzed using Design Expert-12 software and responses were considered significant using ANOVA when probability (P) values were less than 0.05.

The polynomial equation obtained from the design is

$$Y = \beta_0 + \beta_1A_1 + \beta_2B_2 + \beta_3C_3 + \beta_{12} A_1B_2 + \beta_{13}A_1C_3 + \dots\dots\dots\beta_nA_nB_n$$

Where Y is the response of experimental factor  $\beta_0$  is the intercept,  $\beta_1$  to  $\beta_{13}$  is the regression coefficient of respective variables.

2.4.8. Optimization of FEB-NE using BDD

The BDD can be applied for the optimization of NE formulation after the study of responses or variables. The optimization of NE containing FEB was directly determined by graphical and numerical methods [33]. Based on the observations and constraints, the desirability approach was considered for the optimized concentrations of factors followed by analysis using statistical methods. Thereafter, the 3D response surface overlay plot and the contour plot were obtained for the concentration of optimized NE formulation.

2.5. Identification test of FEB-NE

In order to identify the type of NE, the basic identification test such as dilution test, conductivity test, and staining test was performed in triplicates using optimized NE.

2.5.1. Dilution test, staining, and conductivity test

The rationale behind the dilution test of FEB-NE is to assess the cause of instability. Dilution was made in the ratio of 10:1 by adding distilled water to the prepared NE to ensure stability [32,34]. The Lysochrome (diazo dye) was mixed with NE appropriately and examined under the optical microscope. The conductivity test is performed for the electrical conductivity of NE preparation. In order to find out the nature of NE (O/W or W/O), electrical conductivity ( $\sigma$ ) test was performed by a conductivity meter (Systronics, India). The Pt/platinized electrodes were immersed in the NE formulation and electrical conductivity was observed digitally [32].

**Table 2**  
Experimental variables with their actual responses using Box-Behnken Design (BDD).

| Run | Experimental variables          |                                       |                         | Responses               |                           |                                  |
|-----|---------------------------------|---------------------------------------|-------------------------|-------------------------|---------------------------|----------------------------------|
|     | Oil concentration ( $X_1$ ) (%) | $S_{mix}$ concentration ( $X_2$ ) (%) | Amplitude ( $X_3$ ) (%) | *Globule size ( $Y_1$ ) | *Zeta potential ( $Y_2$ ) | *Entrapment efficiency ( $Y_3$ ) |
| 1   | 2.00                            | 1.75                                  | 30                      | 76.54 ± 1.82            | -26.5 ± 1.02              | 89.6 ± 0.01                      |
| 2   | 2.00                            | 1.75                                  | 50                      | 67.91 ± 1.21            | -26.0 ± 1.62              | 87.62 ± 0.12                     |
| 3   | 2.50                            | 2.00                                  | 30                      | 73.20 ± 0.01            | -27.4 ± 1.52              | 90.1 ± 0.32                      |
| 4   | 2.00                            | 2.00                                  | 40                      | 53.83 ± 1.53            | -27.29 ± 1.65             | 86.76 ± 1.01                     |
| 5   | 1.5                             | 1.75                                  | 40                      | 74.88 ± 0.52            | -23 ± 1.05                | 78.32 ± 0.19                     |
| 6   | 2.00                            | 2.25                                  | 50                      | 73.61 ± 0.14            | -31 ± 1.65                | 88.43 ± 1.23                     |
| 7   | 2.00                            | 2.00                                  | 40                      | 53.83 ± 0.65            | -27.29 ± 0.65             | 86.76 ± 1.12                     |
| 8   | 1.50                            | 2.25                                  | 40                      | 49.39 ± 0.65            | -30 ± 0.95                | 93.43 ± 1.74                     |
| 9   | 2.00                            | 2.00                                  | 40                      | 53.83 ± 0.74            | -27.29 ± 1.85             | 86.76 ± 1.52                     |
| 10  | 1.50                            | 2.00                                  | 50                      | 34.85 ± 1.04            | -26.5 ± 1.23              | 83.42 ± 1.20                     |
| 11  | 2.50                            | 2.25                                  | 40                      | 108.5 ± 1.01            | -39.5 ± 1.32              | 94.32 ± 1.02                     |
| 12  | 2.00                            | 2.25                                  | 30                      | 78.40 ± 0.24            | -37.6 ± 0.65              | 86.7 ± 1.08                      |
| 13  | 2.5                             | 1.75                                  | 40                      | 75.48 ± 0.95            | -11.8 ± 0.91              | 91.05 ± 0.52                     |
| 14  | 2.00                            | 2.00                                  | 40                      | 53.83 ± 1.65            | -27.29 ± 1.02             | 86.76 ± 0.35                     |
| 15  | 2.00                            | 2.00                                  | 40                      | 53.83 ± 1.22            | -27.29 ± 1.62             | 86.76 ± 0.81                     |
| 16  | 2.5                             | 2.00                                  | 50                      | 61.77 ± 1.52            | -28.3 ± 1.80              | 92.65 ± 0.14                     |
| 17  | 1.5                             | 2.00                                  | 30                      | 55.41 ± 1.02            | -27.2 ± 0.12              | 84.2 ± 1.65                      |

Coded high values=(-1), Coded middle/mean values=(0), Coded low values=(+1), Maximum alpha values (axial points)= (+ $\alpha$ ), Minimum alpha values (axial points)= (- $\alpha$ ).

The values of responses are presented as mean ± SD, (n = 3); \*Values are measured by dynamic light scattering.

## 2.6. Characterizations of FEB-NE

### 2.6.1. Globule size and PDI

The mean globule size was assessed by a Zeta sizer (Malvern, Worcestershire, UK) instrument. The sample solution was prepared by diluting NE in distilled water in a ratio of 1:100 to avoid multiple scattering. This solution was poured into the disposable cuvette and measured at room temperature. PDI is the width of size distribution in the sample and it was obtained during the measurement of size in triplicates (mean  $\pm$  SD).

### 2.6.2. Zeta potential (ZP)

ZP is the potential difference present between a colloidal particle and the surrounding liquid. This is also known as surface electric charge and the physical stability of the system. The samples of emulsion were diluted suitably using double distilled water and measured by particle sizer (Nano ZS90, Malvern) with electrical conductivity tuned to 50  $\mu$ S/cm. The surface charge (ZP) was calculated using Helmholtz–Smoluchowski equation based on the electrophoretic light scattering technique in triplicates (mean  $\pm$  SD) [35].

### 2.6.3. Entrapment efficiency (EE) and drug loading (DL)

The EE was obtained by the reported minicolumn centrifugation method [36,37]. Briefly, a 10% solution (w/v) of Sephadex® G25 M was prepared in ultra-pure water and kept to swell for over 24 h. On the other hand, minicolumn was prepared using a 1 mL syringe in which a Whatman filter pad was inserted. The swelled Sephadex® G25 M was poured slowly into it and centrifuged for 5 min and 2000 rpm to obtain the packing of gel in the column. Over that the prepared nanoformulation (100  $\mu$ L) was added slowly and centrifuged again using the same speed and time. The emulsion traveled through the gel and eluted globules were further broken using methanol. Subsequently, the sample was diluted and drug (%) was analyzed by taking absorbance at 315 nm spectrophotometrically (Shimadzu 1700, Japan). The untrapped drug was bound to the gel. The drug (%) entrapment was calculated by the mathematical equation

$$\% EE = \frac{A_e}{A_t} \times 100$$

Where  $A_e$  = amount of FEB entrapped and  $A_t$  = total amount of FEB existing in 100  $\mu$ L sample of NE [38].

### 2.6.4. Drug content

The dilution of NE was prepared for the determination of drug content. The dilution in a proportion of 0.1: 100 with methanol was made and absorbance at 315 nm was measured spectrophotometrically [15].

The drug content (%) was calculated by the following formula

$$\text{Drug content (\%)} = \frac{\text{Calculated quantity of FEB in NE}}{\text{Initial quantity of FEB NE}} \times \text{dilution factor} \times 100$$

### 2.6.5. pH and shear viscosity

The pH of FEB-NE was measured by a digital pH meter (ThermoFisher Scientific India Pvt. Ltd., Mumbai, India) by immersing the glass electrode in NE at an ambient temperature [26]. The standard buffers of pH 9.0, 7.0, and 4.0 were used for calibration before use.

The viscosity of optimized NE was determined by RST Cone and Plate Rheometer (Brookfield, Middleborough, USA) with a spindle C50-1 at a temperature of  $25 \pm 0.5$  °C [32,39].

### 2.6.6. Refractive index (RI) and percentage transmittance

Abbes refractometer was used to establish the RI of NE. This study was performed in triplicates [32]. The percent transmittance was determined by spectrophotometrically in which measuring the absorbance of NE at 315 nm without dilution and distilled water was taken as a blank [40].

### 2.6.7. Surface morphology of FEB-NE

**2.6.7.1. Atomic force microscopy (AFM).** Surface morphological information of FEB-NE was investigated by Scanning Probe Microscopy (SPM) integrated by AFM coupled with Raman spectroscopy: TriA 100 (A. P. E. Research Nanotechnology, Italy) coupled with a non-contact cantilever. Freshly prepared NE was diluted in double-distilled water and appropriately spread as a thin film on a mica sheet. The spread samples were kept for air dry for 24 h at room temperature and thereafter, AFM topographic image with 3D view was captured coupled with Gwyddion Software for surface morphological analysis. The instrument was operated using 256.23 Hz frequency in scan mode [41,42].

**2.6.7.2. Transmission electron microscopy (TEM).** TEM was used to evaluate the morphological characteristics of globules such as shape and size. The sample was prepared and deposited a single drop copper grid previously coated with carbon. An aqueous solution of phosphotungstic acid (2% w/v) and uranyl acetate (1% w/v) were used as positive and negative contrast respectively. The image was visualized at an accelerating voltage 200 kV by TEM (Jeol/JEM 2100, Japan) [43].

## 2.7. Stability studies

Accelerated stability studies were performed for an optimized batch of NE for 3 months. The stability temperature and humidity conditions i.e.  $40 \pm 2 \text{ }^\circ\text{C}$  and  $75\% \text{ RH} \pm 5\% \text{ RH}$  were used as per the standard stability guidelines [44]. The optimized FEB-loaded NE was filled into three separate vials and placed for stability studies in a stability chamber (Remi CHM-10S, India). Aliquots of NE were withdrawn at intervals of 0, 45, and 90 days and analyzed for globule size, ZP, and EE [45,46].

## 2.8. In vitro studies and release kinetics

The *in vitro* release study was performed by the dialysis bag (MW 12,000–14,000 Da) technique. In brief, at first, the dialysis bag was soaked overnight in a buffer solution. The FEB-NE (5 mL) was placed in the dialysis bag and tied on two ends of the tube. On the other hand, the FEB suspension was prepared by using 0.5% carboxymethylcellulose and sealed at two ends to avoid leakage. The dialysis bag was immersed in 200 mL buffer solution of pH 1.2 simulated gastric fluid (SGF) followed by pH 6.8 simulated intestinal fluid (SIF) containing SLS (1%) medium maintained at  $37 \pm 0.5 \text{ }^\circ\text{C}$  with continued stirring at 100 rpm [27]. The study was conducted for a period of 24 h (first 2 h in (SGF) and then). The 1 mL sample was withdrawn at 0.5, 1, 2, 4, 8, 12, and 24 h and replaced by the same freshly prepared buffer solution. The FEB-NE and FEB-suspension were examined spectrophotometrically [47].

The release mechanism of the drug was studied by comparing different release kinetic models for FEB-NE and FEB-suspension. For the best-suited mechanism of drug release kinetics, the high correlation coefficient ( $R^2$ ) value was selected.

## 2.9. Permeability study using artificial membrane and everted gut sac

PAMPA study was carried out using the following procedure adopted in our previous paper [27]. The passive permeability was studied using a parallel artificial membrane permeability assay (PAMPA). In this study, the 96-well filter plate was used for the permeation study for FEB-NE and FEB suspension (prepared by 0.5% sod. CMC). A freshly prepared phosphate buffer saline (PBS) solution having pH 6.8 was used throughout the study. BD Gentest coated with a lipid layer was used to obtain permeability of drug. BD Gentest membrane was inserted into a 96-well filter plate having a donor (upper compartment) and acceptor plate (lower compartment). FEB-loaded NE and FEB suspension were diluted in a buffer (pH 6.8) solution to produce the concentration of  $200 \mu\text{g/mL}$ . This solution was filled in all wells in donor compartments. The prepared PBS solution was poured into the receptor compartment at approximately  $300 \mu\text{L}$ . This plate was kept for incubation and after 6 h samples from the donor and receptor were removed and suitably diluted and subsequently analyzed using HPLC. This study was performed three times. The permeability ( $P_e$ ) of the solution was found using the equation given below [48].

$$P_e = -\ln[1 - CA(t)/C_{\text{equilibrium}}]/A \times (1/VD + 1/VA) \times t$$

Where,  $P_e$  indicates permeability (cm/s); A indicates effective area; VD indicates a donor volume, VA indicates receptor volume, t indicates incubation time (s), CD (t) indicates compound concentration in the donor chamber; CA(t) is a compound concentration in receptor chamber, and  $C_{\text{equilibrium}}$  represents the equation  $[CD(t) \times VD + CA(t) \times VA]$ .

In addition, we performed everted intestine sac model method (*ex-vivo*) for complementary support to the PAMPA study. At first, the rats did not have access to water and feed overnight. After scarifying the animals, a small intestine of length  $10 \pm 0.2 \text{ cm}$  was removed and used for permeability study. The excised gut sac was reverted by using a glass rod. It was then washed with water and kept in ice-cold KRB buffer solution. The sac was closed at one end and the sample solution of 1 mL was filled by second end and tied properly. The prepared sac filled with the sample was kept in KBr buffer solution with supply of oxygen at a  $37 \text{ }^\circ\text{C}$  temperature. At the regular interval of time, 0.5 mL volume was withdrawn and replenished to maintain sink condition. The withdrawal sample was suitably diluted and analyzed by UV-visible spectrophotometer in triplicates. The rate of drug transport through the sac over time was calculated to obtain the permeability [10,27].

The permeability ( $P_{\text{app}}$ ) was calculated by following equation,  $P_{\text{app}} = \frac{J}{A \times C_i}$

where, J is designated as permeation flux, A is designated as surface area and  $C_i$  is denoted as initial drug concentration.

## 2.10. In vivo oral bioavailability study

The oral bioavailability study was performed using Wistar male rats approximately weighing 175–185 g. The animal experiment procedure was prepared and approved by Institutional Animal Ethics Committee (IAEC), RCPIPER, Shirpur. All the experiments using animals were performed by following the revised 1923 guidelines NIH publication No. 8023.

For this study, Wistar rats were divided into three cages and each cage having 6 rats. Animals were kept without feed for 12 h before the study. The animal groups were categorized into FEB-NE, control, and FEB-suspension. The animal oral dose was calculated as 10 mg/kg and administered orally through oral gavage to the test group. The control group was administered only vehicle via same route using oral gavage and FEB-suspension (prepared by adding 1% sodium carboxymethyl cellulose) was given to FEB-suspension group. Before this, anesthetic solution composed of mixing ketamine and xylazine in 10:1 proportion was administered to the rats intraperitoneally [49]. The blood samples were withdrawn approximately 2–2.5 mL from retro-orbital plexus at various time points such as 0.5, 1, 2, 4, 8, and 24 h. Blood samples were collected in an eppendorf tube. The samples were mixed thoroughly by a di-sodium EDTA solution to avoid clotting. Further, these Eppendorf tubes were shaken completely followed by ultracentrifuged at 3500 rpm for 15 min

at 4 °C to separate the plasma. The separated plasma was stored in the refrigerator for further analysis [50].

The plasma was precipitated by adding ethyl acetate in 1:3 ratio (plasma: ethyl acetate). The prepared mixture was vortexed properly followed by centrifugation (4000 rpm and 10 min) for separation of supernatant and precipitate. An aliquot was prepared from the separated supernatant and blended with mobile phase and analyzed by HPLC (Waters Alliance 2695 Separation Module) system. The data was obtained from the software (Empower<sup>TM</sup> FR3) installed in Waters HPLC system. Analysis was performed by isocratic separation with a flow rate 1.2 mL/min.

### 2.11. Statistical analysis

All the calculations were performed by the Microsoft excel sheet enabled with PK solver 2.0 software. A non-compartmental study enabled with a trapezoidal technique was studied to evaluate the pharmacokinetic parameters. Graph Pad Prism Ver. 4.0 enabled in Computer was used for the analysis of statistical data. Afterward, Student's *t*-test, one-way ANOVA followed by Dunnett's tests were analyzed and  $P < 0.05$  was considered statistically significant. All the results were written in Mean  $\pm$  SD.

## 3. Results and discussion

The nanoemulsion is an effective delivery system for the lipophilic drug in order to facilitate ease of absorption, permeability, and bioavailability. For the building of quality in the design of nanoemulsion formulation, QbD-based statistical optimization was performed. This formulation was further investigated for physicochemical characterizations, permeability, and bioavailability studies.

### 3.1. Selection of right oil for development of NE

Oil is an important component for the development of NE. The oil facilitates the entrapment of drug inside the globules. Hence it was a crucial step in the development of NE. Captex 200P oil was chosen among the tested oils because it showed the highest solubilization potential for FEB. The solubility behavior of the model drug FEB was displayed in Fig. S2.

### 3.2. Selection of appropriate surfactant for the development of NE

For the development of NE, the selection of proper surfactant is of utmost important for the stabilization. Surfactant reduces the surface Gibbs-free energy and interfacial tension. They act by the mechanism of electrostatic and steric stabilization which results in the inhibition of globule growth [5].

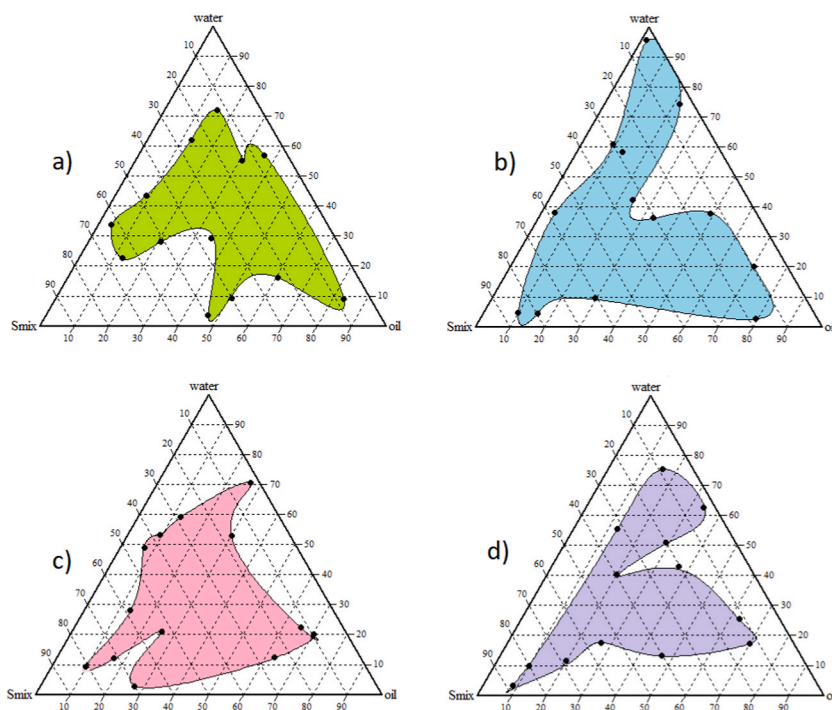


**Fig. 2.** Pseudoternary phase diagram plotted with a) Captex 200P,  $S_{mix}$  (1:1), and water, b) Captex 200P,  $S_{mix}$  (2:1), and water, c) Captex 200P,  $S_{mix}$  (3:1), and water, d) Captex 200P,  $S_{mix}$  (4:1), and water.



Of the various surfactants, Tween 80 possesses the highest solubility of the drug and hence it was screened. The development of the NE with Tween 80 alone reduces the particle size and less stability after keeping a long period. This might be due to insufficient stabilizer required to cover the drug particles [5]. Thereafter, the NE was developed using an appropriate blend of Tween 80 and Lipoid E50 which achieved minimized globule size with stable NE [15].

### 3.3. Preformulation and pseudo-ternary phase diagram for nanoemulsion (NE)

Before the process initiation, the first step was a screening of starting components for the formulation of NE. The screening study for oils and surfactants was performed using the shake-flask method. Captex 200P as potential oil was screened among the oils tested. Tween 80 and Lipoid E 80 were selected as potential surfactants used for stabilization. The higher solubility of drug in the oil and surfactant is a function of entrapment efficiency and drug content.

Further, the appropriate ratio of surfactant-cosurfactant was finalized on the basis of the pseudo-ternary diagram. This diagram was utilized for the determination of the emulsification region and precise  $S_{mix}$  ratio to obtain a clear and stable emulsion. The excipient selected for the preparation of NE should be miscible with each other. The  $S_{mix}$  was prepared by several concentrations (1:9 to 9:1) of Tween 80 and Lipoid E80 as surfactant-cosurfactant. Fig. 2 shows the NE region in the pseudo-ternary phase diagram. This figure represents the minimum NE region for  $S_{mix}$  1:1 and the maximum  $S_{mix}$  region for 2:1 was observed.

The colored portion represents the emulsification region and the uncolored represents turbid region. In this experiment, we took different concentrations of  $S_{mix}$  (1:1, 2:1, 3:1, 4:1). During this process the different emulsification regions (colored) were obtained and this was totally based on aqueous titration [15]. The ratio 2:1 of  $S_{mix}$  was found to be optimum for the NE formation and higher stability was obtained. The three formulations were isolated as optimum for the NE because of higher stability and clarity. The ratio 1:9, 2:8, 3:7 (Oil:  $S_{mix}$  ratio) was found optimum with the proper optimum  $S_{mix}$  ratio 2:1. After the application of stressed conditions such as freeze-thaw cycle, heating-cooling cycles, centrifugation test, the optimum formulation was ensured in a ratio of 3:7 (Oil:  $S_{mix}$  ratio). Thus, this formulation was considered for further study and characterization.

### 3.4. QbD based nutshell

#### 3.4.1. Assignment of QTPP

FEB loaded NE was initiated by assigning QTPP which was the features of drug release, pharmacokinetics, and stability. For the targeting of the QTPP, the optimized quality attributes were identified such as globule size ( $Y_1$ ), ZP ( $Y_2$ ), and EE ( $Y_3$ ) to achieve the desired product. These attributes were selected as response variables in BDD on the basis of various experiments and available literature.

#### 3.4.2. Risk assessment studies

The risk assessment steps were performed using FMEA (Table S2) for the identification of quality risk factors that could be used for the production of NE [51]. The isolated experimental variables were enabled with the highest risk via the ranking-based system. This system directly had an impact on the performance of the formulation. Hence, the isolated CPP i.e. Amplitude (%), CMA i.e. Oil (%), and  $S_{mix}$  (%) were considered as critical based on the RPN score. Thus, amplitude received the highest score to qualify in risk assessment study because it has a unique quality to achieve globule size at nano level. Oil was considered as highest RPN rank due to the high solubility of drug in oil. And due to this reason the drug content, entrapment efficiency, and drug release were efficient. The  $S_{mix}$  concentration stabilized the emulsion for a long time because of surfactant characteristics to prevent aggregation and agglomeration and hence was selected as critical.

#### 3.4.3. Effect of experimental variables using BDD

The design expert suggested different batches of FEB-loaded NE and run simultaneously to assess the effect of responses. The globule size was found in the range required for the NE by the participation of oil, a combination of surfactant, and optimum amplitude. ZP was one of the crucial responses in the design for the stabilization of NE. EE depends on the solubility of drug in oils and was a function of the percent drug successfully entrapped in the globules.

#### 3.4.4. Effect on globule size

The globule size is the response of the experiment depicted in Fig. S3. It ranged from  $34.85 \pm 1.04$  nm to  $108.5 \pm 1.01$  nm for all the batches of BDD. The polynomial equation for globule size ( $Y_1$ ) shows in eq. (1).

$$\text{Globule Size } (Y_1) = 53.83 + 13.05 \times X_1 + 1.89 \times X_2 - 5.68 \times X_3 + 14.63 \times X_1 \times X_2 + 0.96 \times X_2 \times X_3 + 2.71 \times X_1^2 + 20.52 \times X_2^2 - 0.23 \times X_3^2 \dots (1)$$

Globule size has a synergistic relationship with the concentrations of oil and surfactant while an antagonistic relationship with amplitude. It shows a positive combined effect of the concentrations of lipid and surfactant. The above equation shows the positive effect of surfactant concentration and amplitude. Wave energy generated by the probe sonicator had a direct impact on the globules in dispersion. The on-off cycle had a great influence on the reduction of particle size. The wave energy generated a cycle of compression and rarefaction in the emulsion. Propagation of intense shock waves in liquids increases the speed of moving particles inside the liquid and results in micromixing and uniform particles in emulsion. Hence, increase in amplitude increases the surface area of the particle and simultaneously reduces the globule size [52]. Above the optimum level, globule size was slightly increased and this could happen

due to the nucleation which leads to agglomeration [10].

### 3.4.5. Zeta potential (ZP)

ZP is the surface charge on the globule of NE and ranged  $-11.8 \pm 0.91$  to  $-39.5 \pm 1.32$ . The response obtained from the experimental run was depicted in Fig. S3.

The polynomial equation is represented in eq. (2)

$$ZP (Y_2) = -21.38 + 6.81 \times X_1 - 12.98 \times X_2 - 12.61 \times X_3 - 5.17 \times X_1 \times X_2 - 14.10 \times X_1 \times X_3 + 14.77 \times X_2 \times X_3 \dots \quad (2)$$

It shows a positive effect on oil concentration and negative effect of surfactant concentration and a negative relationship with amplitude. ZP has the negative effect of combined concentrations of lipid and surfactant while the negative effect of lipid and amplitude. ZP has a synergistic effect on combined surfactant concentration and amplitude. ZP enhances the stability of the emulsion. Hence ZP was the critical attribute in the development of the NE.

NE is thermodynamically unstable and can have a ZP value  $\pm 30$  mV. In current work the ZP of NE coupled with nanosized globules showed between  $-11.8 \pm 0.91$  to  $-39.5 \pm 1.32$  mV indicating stable system due to negative surface charge around the globules. But high ZP value (Table 2) of FEB-NE system suggesting thermodynamically stable that renders difficulty in separation due to electric repulsion.

### 3.4.6. Entrapment efficiency (EE)

EE had a positive effect on oil, surfactant, and amplitude. The result obtained for entrapment efficiency was shown in Fig. S3 and was found to be in the range of  $78.32 \pm 0.19$  to  $94.32 \pm 1.02$ . The polynomial equation is depicted in eq. (3).

$$EE (Y_3) = 87.86 + 3.59 \times X_1 + 2.04 \times X_2 + 0.19 \times X_3 \quad (3)$$

The figure depicted a contour and response surface plot indicating the effect of experimental variables on entrapment efficiency and level of significance was considered ( $p$ -value  $> 0.05$ ). The strong positive effect of oil mixture is due to its highest capacity to solubilize the drug, FEB. At the same time drug shows emulsification capacity in the optimum ratio of  $S_{mix}$  which was finalized by the pseudo-ternary phase diagram. The amplitude had a synergistic effect on the entrapment of drug. The entrapment also strengthens by the stabilization of emulsion using a combination of surfactant and oil.

### 3.4.7. Statistical optimization of NE

BDD depicted the experimental variables and their various responses (Table 2). The experimental variables with their levels and the constraints of various responses are displayed in Table S3. The experimental variables were studied as a function of globule size, ZP, and EE. Results of ANOVA for the responses are displayed in Table 3 and best-fitted models and fit summary statistics are depicted in Table S4.

The response surface methodology was employed for optimal formulation. Using numerical and graphical optimization method the 3D overlay plot region and contour region was obtained which indicates design space (Fig. 3). The obtained desirability value 0.706 (nearest to 1) was selected for optimized NE. The optimized FEB-NE was prepared using obtained set of concentrations of experimental variables. The results were compared with predicted values and the calculated error (%) was depicted in Table 4.

### 3.4.8. Identification test (dilution, staining, and conductivity test)

An optimized FEB-loaded NE was clear and transparent solution. No signal of instability of NE was observed. Thus, the present FEB-loaded NE was said to be oil in water (O/W) NE. A staining test was performed using oil-soluble dye. The optimized NE showed colorless background and red-colored oil globules. The electrical conductivity power of NE is increased as the water content increases. Thus, the NE was identified as o/w type of emulsion.

**Table 3**

ANOVA for responses measurement of particle size, zeta potential and entrapment efficiency.

| Source  | Sum of squares | df | Mean square | F-value | p-value |             |
|---|----------------|----|-------------|---------|---------|-------------|
| <b>Response 1: Particle size (Y1)</b>         |                |    |             |         |         |             |
| Quadratic Model                               | 4367.92        | 9  | 485.32      | 47.69   | 0.0001  | Significant |
| Residual                                      | 71.23          | 7  | 10.18       |         |         |             |
| Cor Total                                     | 4439.15        | 16 |             |         |         |             |
| <b>Response 2: Zeta potential (Y2)</b>        |                |    |             |         |         |             |
| 2FI Model                                     | 4766.25        | 6  | 794.38      | 7.48    | 0.0030  | Significant |
| Residual                                      | 1062.36        | 10 | 106.24      |         |         |             |
| Cor Total                                     | 5828.61        | 16 |             |         |         |             |
| <b>Response 3: Entrapment efficiency (Y3)</b> |                |    |             |         |         |             |
| Linear Model                                  | 136.78         | 3  | 45.59       | 5.44    | 0.0121  | Significant |
| Residual                                      | 109.04         | 13 | 8.39        |         |         |             |
| Cor Total                                     | 245.82         | 16 |             |         |         |             |

df - Degree of freedom, F - Fisher's ratio, and  $p$ -probability.

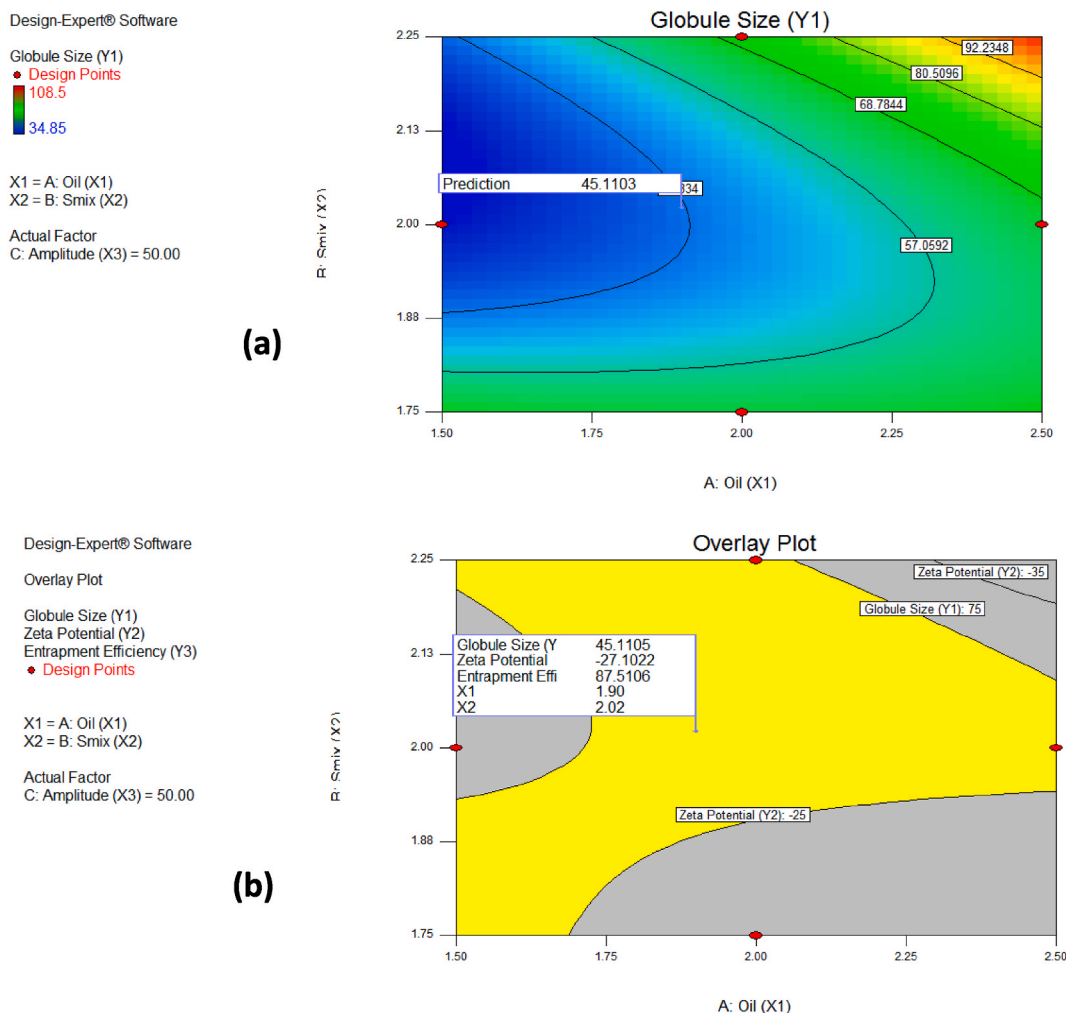


Fig. 3. Optimization of formulation with (a) Contour region and (b) 3D overlay plot region.

Table 4

An optimized FEB-NE showing predicted and observed responses.

| Formulation variables | Oil concentration (X <sub>1</sub> ) (%) | Smix concentration (X <sub>2</sub> ) (%) | Amplitude (X <sub>3</sub> ) (%) |
|-----------------------|---|--|---------------------------------|
| Concentrations        | 1.9                                     | 2.02                                     | 50                              |
| Responses             | Globule size (Y <sub>1</sub> )          | ZP (Y <sub>2</sub> )                     | EE (Y <sub>3</sub> )            |
| Predicted mean        | 45.11                                   | -27.10                                   | 87.51                           |
| # Observed mean       | 47.84 ± 0.14                            | -25.86 ± 1.36                            | 89.88 ± 0.23                    |
| *Error (%)            | 6.05                                    | 4.57                                     | 2.70                            |

ZP, Zeta potential; EE, Entrapment efficiency. # Values indicates mean ± SD (n = 3).

\*Error (%) = (actual value - predicted value)/predicted value × 100.

### 3.4.9. Drug content and drug loading

The drug content was calculated to be 94.73% ± 1.23%. It indicates the total amount actual drug (%) present in formulated NE. The drug loading was analyzed by UV spectrophotometrically and calculated to be 0.45 mg/mL.

### 3.4.10. pH, and shear viscosity

The pH of optimized NE was found to be 7.2 ± 0.2. This pH of NE is suitable for oral emulsion and would not be physiologically irritant. The NE has an important characteristic such as low viscosity related to stability. FEB-NE was transparent and it was necessary to measure the viscosity. The viscosity 48.25 ± 1.54 mPas of the prepared NE was obtained.

### 3.4.11. Refractive index (RI) and percent transmittance

A drop of FEB-NE (without dilution) was applied in the chamber of Abbe's refractometer at  $25 \pm 1$  °C to determine the RI. The refractometer displayed the RI value  $1.232 \pm 0.102$  confirming the transparent FEB-NE and showed the isotropic nature as an additional characteristic.

After analyzing the optimized NE using spectrophotometrically, the calculated percentage transmittance observed was  $98.19 \pm 0.03\%$ . It indicates that the formulation was clear and transparent provided that the observed value was closed to 100%.

## 3.5. Surface morphology

### 3.5.1. AFM

The morphological characteristics of globules were captured by AFM (Fig. 4). The shape of FEB-NE was found nearly spherical and size range maximum 92.5 nm slightly larger than the optimized NE batch. This is due to the tip-broadening effect when the cantilever tip was in contact with soft materials [41]. A maximum height 73.29 nm was found which appeared similar to the mountain due to clusters of globules.

### 3.5.2. HR-TEM

The HR-TEM image was displayed in Fig. 5. The nanoglobule was observed for TEM image which is equivalent to the globule measurement by DLS method (Zeta sizer, Nano ZS90, Worcestershire, UK). Nanoglobules were observed as dark spherical shape with a globule size below 100 nm. Thus, it was confirmed that the formulated emulsion was NE [53].

## 3.6. Stability

Under standard storage conditions of stability testing of new drug substances and suggested by ICH, the NE containing FEB was observed for 90 days. The NE was observed as stable physically and chemically. Table 5 shows the results of stability studies for 90 days for critical attributes of NE such as globule size, dispersity, ZP, and EE. No color change or phase separation were observed during the study.

The globule size after 90 days increased which was found statistically significant (Unpaired student t-test,  $p < 0.05$ ). Similarly, dispersity was changed significantly upon storage for long duration of time (Unpaired student t-test,  $p < 0.05$ ). It was observed NE was stable up to the 4 months and might have the possibility of aggregation of globule upon long term. However, ZP, and EE did not change significantly upon storage (Unpaired student t-test,  $p > 0.05$ ).

## 3.7. In vitro release study

In order to achieve the bioavailability of poorly soluble FEB, the NE is the best system. The drug was encapsulated into a nanosized globule to enhance the drug release and better therapeutic results. *In vitro* drug release behavior of FEB-NE and FEB-suspension was performed at 1.2 pH for the first 2 h followed by 6.8 pH buffer (Fig. 6). The *in vitro* studies showed 93.32% drug release for FEB-loaded NE and 43.23% for FEB suspension (Fig. 6).

The mechanism of release behavior for FEB-NE and FEB-suspension was studied using different kinetic models such as Zero order, First order, Korsmeyer–Peppas, Higuchi-matrix, and Hixson-Crowell [38].

The mechanism of release kinetics was observed and found to be 'Higuchi-matrix' as a best-suited model for the FEB-NE and FEB-suspension based on a comparison study of all release kinetic behaviors. The regression coefficient was obtained to be 0.9236 ( $R^2$ ) (Table 6).

The maximum drug release was obtained from the optimized NE due to the nanosized globules which increases the surface area of globules for diffusion. Similar results were obtained in previous study published by Gokhale et al. [32]. Thus, NE shows the controlled release behavior in simulated physiological conditions.

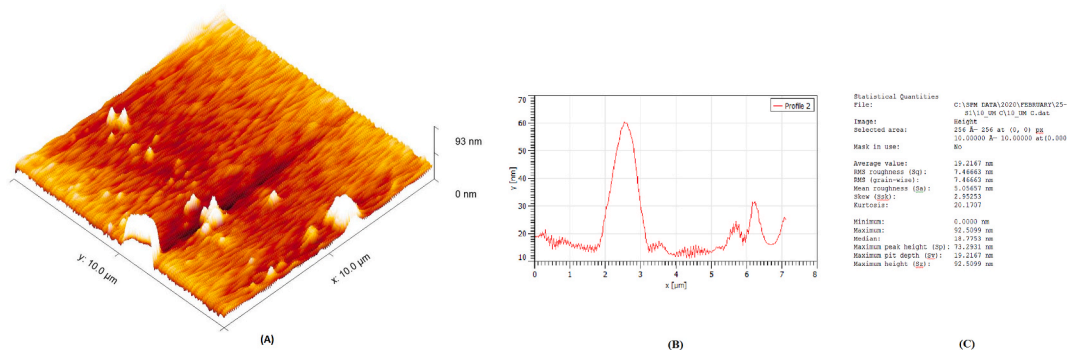


Fig. 4. Photomicrograph of atomic force microscopy (AFM) with 3D view (A), profile of globule size (B), statistical quantities (C).

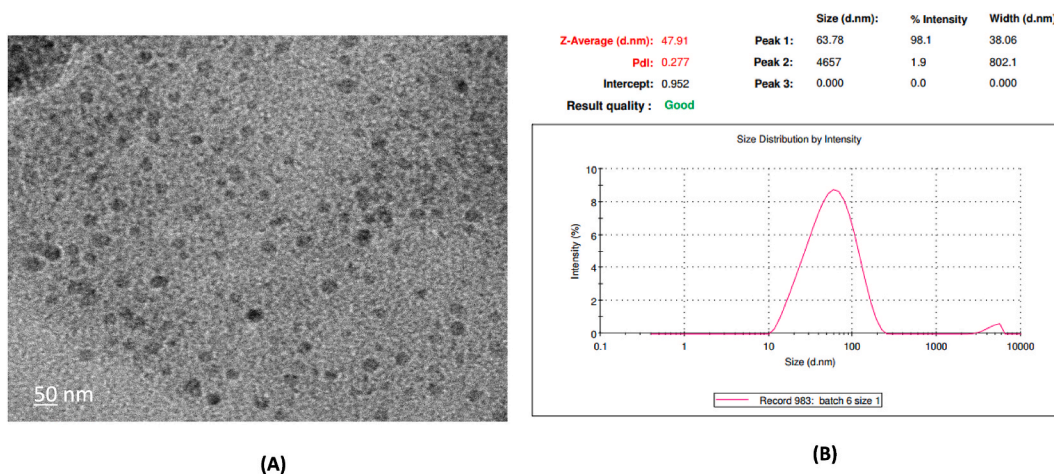


Fig. 5. Transmission electron microscopy (TEM) analysis (A) and globule size measurement by DLS method (B).

Table 5  
Stability studies for optimized FEB-NE.

| Parameters          | Measurement on 1st Month |                 | Measurement after 4th month |                 | Measurement after 6th month |                 |
|---------------------|--------------------------|-----------------|-----------------------------|-----------------|-----------------------------|-----------------|
|                     | 4 °C                     | 25 °C           | 4 °C                        | 25 °C           | 4 °C                        | 25 °C           |
| Physical appearance | No color change          | No color change | No color change             | No color change | No color change             | No color change |
| Phase separation    | No                       | No              | No                          | No              | No                          | No              |
| Globule size        | 42.23 ± 1.00             | 43.56 ± 1.03    | 49.66 ± 0.262               | 50.26 ± 0.83    | 53.25 ± 0.75                | 55.81 ± 0.76    |
| Dispersity          | 0.126 ± 0.02             | 0.158 ± 0.03    | 0.259 ± 0.07                | 0.289 ± 0.01    | 0.289 ± 0.02                | 0.245 ± 0.02    |
| *ZP                 | -12.09 ± 0.31            | -13.03 ± 0.55   | -13.87 ± 0.50               | -13.59 ± 0.35   | -13.86 ± 0.52               | -13.96 ± 0.37   |
| **EE                | 89.36 ± 0.41             | 89.76 ± 0.12    | 89.36 ± 1.03                | 88.12 ± 1.22    | 88.24 ± 0.54                | 87.02 ± 0.21    |

\*Zeta potential and \*\*Entrapment efficiency.

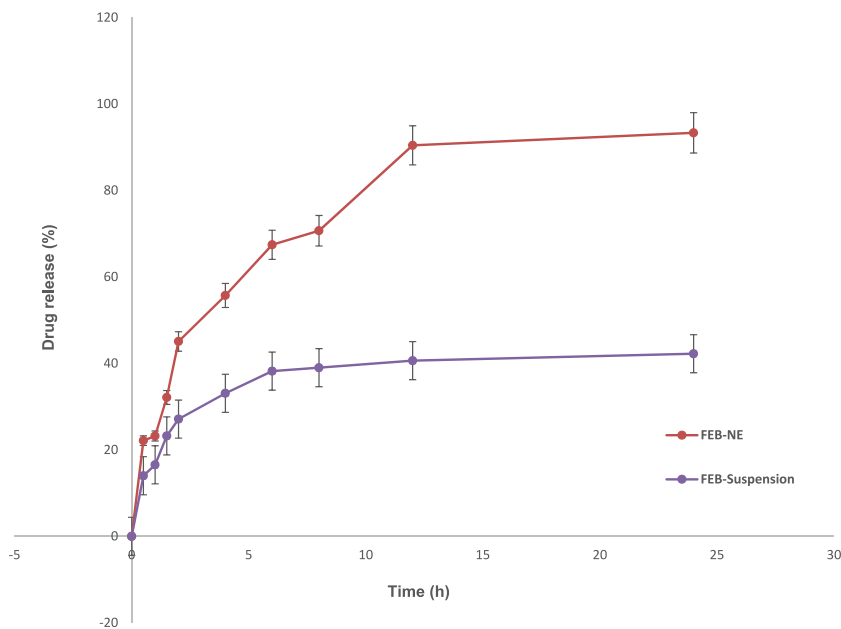


Fig. 6. Cumulative amounts of drug release profiles of optimized FEB-NE and FEB-suspension.

**Table 6**  
Comparison of drug release kinetics model.

| Batch code     | Drug release kinetics model |            |                    |                |                |
|----------------|-----------------------------|------------|--------------------|----------------|----------------|
|                | First order                 | Zero order | Korsemeyer- Peppas | Higuchi-matrix | Hixson-Crowell |
| FEB-NE         | 0.9028                      | 0.7093     | 0.8948             | <b>0.9236</b>  | 0.8539         |
| FEB-Suspension | 0.571                       | 0.5188     | 0.6905             | 0.7995         | 0.5537         |

“r<sup>2</sup>” represents correlation coefficient.

In this study, initial fast release for first 2 h followed by sustained release from NE was observed. On the other hand, FEB-suspension shows very slow release and it could be due to lack of surfactant and drug's own characteristic i.e. poor solubility. Moreover, the composition of NE was oil which has highest solubility of drug showed a controlled manner of release from the nanoformulation. In addition, surfactant (Tween 80) is part of the composition and facilitates to reduce the globule size which can absorb quickly. During the preparation of NE, the model drug FEB was encapsulated in oil and surfactant which results in slow and sustained manner release behavior to achieve desired effect.

### 3.8. PAMPA study and everted gut sac permeability method

The PAMPA study was used to find the permeability of the FEB across the transcellular mechanism of passive diffusion. The drug has adequate lipophilicity in order to access the drug in systematic circulation. This is low-cost, robust, and reproducible permeability study having high efficacy. The literature search revealed that no such passive permeability test was conducted for FEB-NE. The comparison of NE and Drug-suspension has been observed and permeability has been increased by 2.72 fold (Table 7). It was found that the improved permeability of NE due to the nanosizing and composition facilitates the opportunity for the permeability with the formulations. The absorption and permeability were due to the reduced size of globules and surfactant (Tween 80) employed for development of NE [54]. It has been noted that the absorption site was due to the drug's enhanced solubility and GI environment. Most importantly, the enhanced permeability was due to the amorphous drug encapsulated in globules.

Further, in order to support the PAMPA study we performed everted sac study in order to mimic the permeability of drug across the intestine on FEB-NE and FEB suspension. Subsequently, it was observed that the permeability of NE has been increased as compared to the FEB-suspension. Table 7 shows that NE has been increased 2.54 fold. Thus, the increase in permeability was due to the nanosizing of drug encapsulated in globules. It could be due to the combined effect of surfactant and co-surfactant used in the development of NE.

PAMPA study always complements for the everted gut sac study with a proper correlation which provides valuable, reproducible, and robust results associated with the permeability of formulation. Thus, improved permeability was observed in both studies i.e. passive permeability and responsible for the absorption and enhanced bioavailability [10].

### 3.9. In vivo drug release mechanistic study

*In vivo* study was performed to find out the pharmacokinetic performance of drug entrapped in globules of novel synthesized FEB-NE which were assessed using PK solver software. The linearity equation was used to find out the drug concentration in plasma employing the estimated and validated HPLC method. The plot between plasma concentrations ( $\mu\text{g}/\text{mL}$ ) versus time was observed after oral administration of FEB-NE (Fig. 7). The pharmacokinetic parameters for oral administration of FEB-NE are displayed in Table 8. A pharmacokinetic study showed an improvement in oral bioavailability 2.48 folds as compared to FEB-suspension. A pharmacokinetic study showed the comparison between optimized FEB-NE, Control, and FEB-suspension group (Fig. 7), and the observations are displayed in Table 8.

1.  $C_{\text{max}}$  was higher in case of optimized FEB-NE ( $0.491 \pm 1.31$ ) than FEB-suspension ( $0.197 \pm 1.03$ ) suggesting that higher oral absorption of FEB from the NE.  $\text{AUC}_{0-t}$  ( $2.105 \pm 1.04 \mu\text{g}/\text{mL} \cdot \text{h}$ ) was less in case of FEB-suspension than FEB-NE showing  $\text{AUC}_{0-t}$  ( $5.239 \pm 2.15 \mu\text{g}/\text{mL} \cdot \text{h}$ ) which indicates an enhanced higher concentration of drug in the systemic circulation. The observation shows that the improvement in the bioavailability of model lipophilic drug FEB and relative bioavailability was obtained 284%. It means 2.48 fold increase in the bioavailability of optimized FEB-NE as compared to FEB-suspension.
2. During the NE production process the globule size reduced up to nano-level. Due to the reduced size and higher absorption rate, enhanced the plasma drug concentration of FEB-NE which results in improved bioavailability. Moreover, FEB-NE observed the controlled release of drug throughout the experiment.
3. Small and nano-range globule is equally important for absorption and improved bioavailability. Due to the reduced globule size, it could be bypassed the liver metabolism. In addition, the easy absorption of FEB was observed due to the non-ionic surfactant (Tween 80) which was used in our previous publications [27,30]. Ease of absorption enhances the drug transport through the lymphatics which results in improved bioavailability.
4. The mean residence time (MRT) value of FEB-NE was found higher as compared to drug suspension (Table 8). It indicates the circulation time was improved from the developed FEB-NE in comparison to drug suspension. Thus, a significant difference was observed for MRT values. Thus, the pharmacokinetic study revealed improved bioavailability of FEB encapsulated in nanoemulsion systems.

**Table 7**  
Permeability studies of optimized FEB-NE and FE-suspension.

| Permeability values | Formulations     |                 |
|---------------------|------------------|-----------------|
|                     | Optimized FEB-NE | FEB-Suspension  |
| $P_e$               | $1.96 \pm 0.02$  | $0.72 \pm 0.06$ |
| $P_{app}$           | $1.78 \pm 0.04$  | $0.70 \pm 0.03$ |

$P_e$  and  $P_{app}$  are the permeability (effective) and apparent permeability respectively.

**Table 8**  
Pharmacokinetic profile of Control, FEB-Suspension and optimized FEB-NE in rat plasma.

| Parameters  | Control          | EEB-Suspension   | FEB-NE           |
|---|------------------|------------------|------------------|
| $T_{max}$ (h)   | 2                | 4                | 4                |
| $C_{max}$ ( $\mu\text{g}/\text{mL}^*\text{h}$ )       | $0.127 \pm 0.16$ | $0.197 \pm 1.03$ | $0.491 \pm 1.31$ |
| AUC 0-t ( $\mu\text{g}/\text{mL}^*\text{h}$ )         | $2.079 \pm 1.12$ | $2.105 \pm 1.04$ | $5.239 \pm 2.15$ |
| AUC 0- $\infty$ ( $\mu\text{g}/\text{mL}^*\text{h}$ ) | $2.107 \pm 1.25$ | $3.40 \pm 1.23$  | $5.22 \pm 2.32$  |
| MRT (h)   | 11.12            | 12.63            | 18.28            |
| Relative bioavailability                              | –                | –                | 248%             |

Values are represented as mean  $\pm$  SD (n = 3).  $T_{max}$ , Time to peak drug concentration;  $C_{max}$ , maximum concentration; AUC 0-t, area under the concentration-time curve; AUC 0- $\infty$ , area under curve to infinite time; MRT, mean residence time. One-way ANOVA and Dunnett's tests were applied to analyze the data (significance level  $p < 0.05$ ).

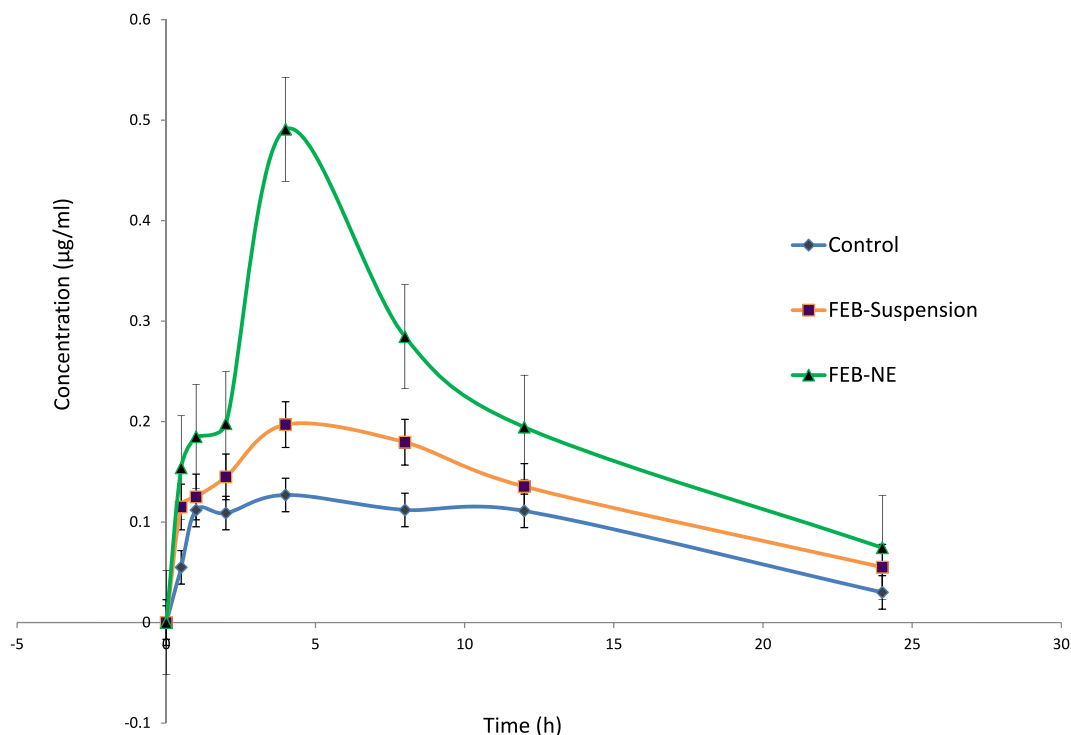


**Fig. 7.** Plasma concentrations versus time profile after oral administration of optimized FEB-NE and FEB-suspension.

#### 4. Conclusion

Thus, the FEB-NE was developed successfully by implementing QbD based approach. The experimental variables were identified by the Ishikawa diagram and subsequently, potential failure modes of variables were detected based on RPN score. The quality and stability of emulsion depend on the appropriate choice of surfactant and co-surfactant combination. In the present study, the ternary phase diagram was constructed to select an area of FEB-NE using the proper combination of stabilizers. The FEB-NE was optimized using BDD which renders the effect of experimental variables on their response. The optimized formulation showed a spherical shape and uniform globule size depicted by AFM and TEM. The FEB-NE showed sustained release behavior and was stable for 90 days under

standard storage conditions. The enhanced permeability was shown by PAMPA and everted sac method subsequently. The pharmacokinetic study revealed the bioavailability successfully improved by 2.48 folds. Thus, FEB-NE is the best option for oral delivery in order to manage chronic gout conditions. The QbD based development of FEB-NE proved the economic and time-saving product and can be a brilliant delivery system for FEB. Thus, NE can be produced on an industrial scale and has a large scope for development in future.

#### Author contribution statement

Vishal Gurumukhi; Shailesh Subhashrao Chalikwar: Conceived and designed the experiments; Wrote the paper.  
Vivek Sonawane: Performed the experiments; Analyzed and interpreted the data.  
Ganesh Tapadiya; Sanjaykumar Bari; Sanjay Surana: Contributed reagents, materials, analysis tools or data.

#### Data availability statement

Data will be made available on request.

#### Declaration of competing interest

The authors declare no conflict of interest.

#### Acknowledgement

This research was supported by 'Special Research Fund' (SYIPER/Mgt-fund/Research/2019/06) from the management of Shreeyash Pratishtan, Aurangabad, and Shirpur Education Society, Shirpur. The authors thank to the Principal and HOD for the support of the research facility.

#### Appendix A. Supplementary data

Supplementary data to this article can be found online at <https://doi.org/10.1016/j.heliyon.2023.e15404>.

#### References

- [1] D.M. Darandale, K.B. Erande, S.R. Tambe, R.S. Bhamber, Development and validation of RP-HPLC method for the determination of febuxostat in bulk and pharmaceutical dosage form, *Asian J. Res. Chem.* 10 (2017) 713, <https://doi.org/10.5958/0974-4150.2017.00121.3>.
- [2] D. Maddileti, S.K. Jayabun, A. Nangia, Soluble cocrystals of the xanthine oxidase inhibitor febuxostat, *Cryst. Growth Des.* 13 (2013) 3188–3196, <https://doi.org/10.1021/cg400583z>.
- [3] S. Singh, P. Parashar, J. Kanoujia, I. Singh, S. Saha, S.A. Saraf, Transdermal potential and anti-gout efficacy of Febuxostat nanosomal gel, *J. Drug Deliv. Sci. Technol.* 39 (2017) 348–361, <https://doi.org/10.1016/j.jddst.2017.04.020>.
- [4] M.A. Martillo, L. Nazzal, D.B. Crittenden, The crystallization of monosodium urate, *Curr. Rheumatol. Rep.* 16 (2014), <https://doi.org/10.1007/s11926-013-0400-9>.
- [5] B.K. Ahuja, S.K. Jena, S.K. Paidi, S. Bagri, S. Suresh, Formulation, optimization and in vitro-in vivo evaluation of febuxostat nanosuspension, *Int. J. Pharm.* 478 (2015) 540–552, <https://doi.org/10.1016/j.ijpharm.2014.12.003>.
- [6] A.M. Vohra, C.V. Patel, P. Kumar, H.P. Thakkar, Development of dual drug loaded solid self microemulsifying drug delivery system: exploring interfacial interactions using QbD coupled risk based approach, *J. Mol. Liq.* 242 (2017) 1156–1168, <https://doi.org/10.1016/j.molliq.2017.08.002>.
- [7] D. Guimarães, A. Cavaco-Paulo, E. Nogueira, Design of liposomes as drug delivery system for therapeutic applications, *Int. J. Pharm.* 601 (2021), <https://doi.org/10.1016/j.ijpharm.2021.120571>.
- [8] S. Shafiq, F. Shakeel, S. Talegaonkar, F.J. Ahmad, R.K. Khar, M. Ali, Development and bioavailability assessment of ramipril nanoemulsion formulation, *Eur. J. Pharm. Biopharm.* 66 (2007) 227–243, <https://doi.org/10.1016/j.ejpb.2006.10.014>.
- [9] O.P. Sharma, V. Patel, T. Mehta, Design of experiment approach in development of febuxostat nanocrystal: application of Soluplus® as stabilizer, *Powder Technol.* 302 (2016) 396–405, <https://doi.org/10.1016/j.powtec.2016.09.004>.
- [10] P. Shekhawat, V. Pokharkar, Risk assessment and QbD based optimization of an Eprosartan mesylate nanosuspension: in-vitro characterization, PAMPA and in-vivo assessment, *Int. J. Pharm.* 567 (2019), 118415, <https://doi.org/10.1016/j.ijpharm.2019.06.006>.
- [11] K.B. Sutradhar, S. Khatun, I.P. Luna, Increasing possibilities of nanosuspension, *J. Nanotechnol.* 2013 (2013), <https://doi.org/10.1155/2013/346581>.
- [12] H. Mu, R. Holm, A. Mullertz, Lipid-based formulations for oral administration of poorly water-soluble drugs, *Int. J. Pharm.* 453 (2013) 215–224, <https://doi.org/10.1016/j.ijpharm.2013.03.054>.
- [13] R. Muzzalupo, L. Tavano, Niosomal drug delivery for transdermal targeting: recent advances, *Res. Rep. Transdermal Drug Deliv.* 23 (2015), <https://doi.org/10.2147/rrtd.s64773>.
- [14] N. Anton, J.P. Benoit, P. Saulnier, Design and production of nanoparticles formulated from nano-emulsion templates-A review, *J. Contr. Release* 128 (2008) 185–199, <https://doi.org/10.1016/j.jconrel.2008.02.007>.
- [15] R. Iqbal, S. Ahmed, G.K. Jain, D. Vohora, Design and development of letrozole nanoemulsion: a comparative evaluation of brain targeted nanoemulsion with free letrozole against status epilepticus and neurodegeneration in mice, *Int. J. Pharm.* 565 (2019) 20–32, <https://doi.org/10.1016/j.ijpharm.2019.04.076>.
- [16] G.M. Patel, P.K. Shelat, A.N. Lalwani, QbD based development of proliposome of lopinavir for improved oral bioavailability, *Eur. J. Pharmaceut. Sci.* 108 (2017) 50–61, <https://doi.org/10.1016/j.ejps.2016.08.057>.
- [17] D. Arora, S. Nanda, Quality by design driven development of resveratrol loaded ethosomal hydrogel for improved dermatological benefits via enhanced skin permeation and retention, *Int. J. Pharm.* 567 (2019), 118448, <https://doi.org/10.1016/j.ijpharm.2019.118448>.
- [18] A. Kovács, S. Berkó, E. Csányi, I. Csóka, Development of nanostructured lipid carriers containing salicylic acid for dermal use based on the Quality by Design method, *Eur. J. Pharmaceut. Sci.* 99 (2017) 246–257, <https://doi.org/10.1016/j.ejps.2016.12.020>.



- [19] N. Rangaraj, S.R. Pailla, S. Shah, S. Prajapati, S. Sampathi, QbD aided development of ibrutinib-loaded nanostructured lipid carriers aimed for lymphatic targeting: evaluation using chylomicron flow blocking approach, *Drug Deliv. Transl. Res.* (2020), <https://doi.org/10.1007/s13346-020-00803-7>.
- [20] E. Pallagi, R. Ambrus, P. Szabó-Révész, I. Csóka, Adaptation of the quality by design concept in early pharmaceutical development of an intranasal nanosized formulation, *Int. J. Pharm.* 491 (2015) 384–392, <https://doi.org/10.1016/j.ijpharm.2015.06.018>.
- [21] I. Conference, O.N. Harmonisation, O.F. Technical, R. For, R. Of, P. For, H. Use, *International Conference on Harmonisation (ICH) of Technical Requirement for Registration of Pharmaceuticals for Human Use, Pharmaceutical Development, Q8 (R2), ICH, 2009, p. 8.*
- [22] ICH guideline Q2(R1), ICH Harmonised Tripartite Guideline, Validation of Analytical Procedures: Text and Methodology, 2005. [http://www.ich.org/fileadmin/Public\\_Web\\_Site/ICH\\_Products/Guidelines/Quality/Q2\\_R1/Step4/Q2\\_R1\\_Guideline.pdf](http://www.ich.org/fileadmin/Public_Web_Site/ICH_Products/Guidelines/Quality/Q2_R1/Step4/Q2_R1_Guideline.pdf).
- [23] M. Joshi, S. Pathak, S. Sharma, V. Patravale, Design and in vivo pharmacodynamic evaluation of nanostructured lipid carriers for parenteral delivery of artemether: nanoject, *Int. J. Pharm.* 364 (2008) 119–126, <https://doi.org/10.1016/j.ijpharm.2008.07.032>.
- [24] J. Desai, H. Thakkar, Enhanced oral bioavailability and brain uptake of Darunavir using lipid nanoemulsion formulation, *Colloids Surf., B* 175 (2019) 143–149, <https://doi.org/10.1016/j.colsurfb.2018.11.057>.
- [25] M. Joshi, V. Patravale, Nanostructured lipid carrier (NLC) based gel of celecoxib, *Int. J. Pharm.* 346 (2008) 124–132, <https://doi.org/10.1016/j.ijpharm.2007.05.060>.
- [26] R. Iqbal, S. Ahmed, G.K. Jain, D. Vohora, Design and development of letrozole nanoemulsion: a comparative evaluation of brain targeted nanoemulsion with free letrozole against status epilepticus and neurodegeneration in mice, *Int. J. Pharm.* 565 (2019) 20–32, <https://doi.org/10.1016/j.ijpharm.2019.04.076>.
- [27] V.C. Gurumukhi, S.B. Bari, Development of ritonavir-loaded nanostructured lipid carriers employing quality by design (QbD) as a tool: characterizations, permeability, and bioavailability studies, *Drug Deliv. Transl. Res.* (2021), <https://doi.org/10.1007/s13346-021-01083-5>.
- [28] S. Shafiq-un-Nabi, F. Shakeel, S. Talegaonkar, J. Ali, S. Baboota, A. Ahuja, R.K. Khar, M. Ali, Formulation development and optimization using nanoemulsion technique: a technical note, *AAPS PharmSciTech* 8 (2007), <https://doi.org/10.1208/pt0802028>. E12–E17.
- [29] N.K. Garg, G. Sharma, B. Singh, P. Nirbhavane, R.K. Tyagi, R. Shukla, O.P. Katare, Quality by Design (QbD)-enabled development of aceclofenac loaded-nanostructured lipid carriers (NLCs): an improved dermatokinetic profile for inflammatory disorder(s), *Int. J. Pharm.* 517 (2017) 413–431, <https://doi.org/10.1016/j.ijpharm.2016.12.010>.
- [30] V.C. Gurumukhi, S.B. Bari, Fabrication of efavirenz loaded nano-formulation using quality by design (QbD) based approach: exploring characterizations and in vivo safety, *J. Drug Deliv. Sci. Technol.* 56 (2020), 101545, <https://doi.org/10.1016/j.jddst.2020.101545>.
- [31] A. Azeem, M. Rizwan, F.J. Ahmad, Z. Iqbal, R.K. Khar, M. Aqil, S. Talegaonkar, Nanoemulsion components screening and selection: a technical note, *AAPS PharmSciTech* 10 (2009) 69–76, <https://doi.org/10.1208/s12249-008-9178-x>.
- [32] J.P. Gokhale, H.S. Mahajan, S.S. Surana, Quercetin loaded nanoemulsion-based gel for rheumatoid arthritis: in vivo and in vitro studies, *Biomed. Pharma* 112 (2019), 108622, <https://doi.org/10.1016/j.biopha.2019.108622>.
- [33] K. Thakur, A. Mahajan, G. Sharma, B. Singh, K. Raza, S. Chhibber, O.P. Katare, Implementation of Quality by Design (QbD) approach in development of silver sulphadiazine loaded egg oil organogel: an improved dermatokinetic profile and therapeutic efficacy in burn wounds, *Int. J. Pharm.* 576 (2020), 118977, <https://doi.org/10.1016/j.ijpharm.2019.118977>.
- [34] M. Laxmi, A. Bhardwaj, S. Mehta, A. Mehta, Development and characterization of nanoemulsion as carrier for the enhancement of bioavailability of artemether, *Artif. Cells, Nanomedicine Biotechnol* 43 (2015) 334–344, <https://doi.org/10.3109/21691401.2014.887018>.
- [35] A. Singh, Y.R. Neupane, B. Mangla, K. Kohli, Nanostructured lipid carriers for oral bioavailability enhancement of exemestane: formulation design, in vitro, ex vivo, and in vivo studies, *J. Pharmaceut. Sci.* 108 (2019) 3382–3395, <https://doi.org/10.1016/j.xphs.2019.06.003>.
- [36] Y. Chen, Q. Wu, Z. Zhang, L. Yuan, X. Liu, L. Zhou, Preparation of curcumin-loaded liposomes and evaluation of their skin permeation and pharmacodynamics, *Molecules* 17 (2012) 5972–5987, <https://doi.org/10.3390/molecules17055972>.
- [37] N.S. Ranpise, S.S. Korabu, V.N. Ghodake, Second generation lipid nanoparticles (NLC) as an oral drug carrier for delivery of lercanidipine hydrochloride, *Colloids Surf., B* 116 (2014) 81–87, <https://doi.org/10.1016/j.colsurfb.2013.12.012>.
- [38] D.D. Kumbhar, V.B. Pokharkar, Engineering of a nanostructured lipid carrier for the poorly water-soluble drug, bicalutamide: physicochemical investigations, *Colloids Surfaces A Physicochem. Eng. Asp.* 416 (2013) 32–42, <https://doi.org/10.1016/j.colsurfa.2012.10.031>.
- [39] N. Riquelme, R.N. Zúñiga, C. Arancibia, Physical stability of nanoemulsions with emulsifier mixtures: replacement of tween 80 with quillaja saponin, *Lwt* 111 (2019) 760–766, <https://doi.org/10.1016/j.lwt.2019.05.067>.
- [40] Nanosuspension of efavirenz for improved oral bioavailability: Formulation optimization, in vitro, in situ and in vivo evaluation, Patel, G. V., Patel, V. B., Pathak, A., & Rajput, S. J. G. V. Patel, V. B. Patel, A. Pathak, S. J. Rajput, Nanosuspension of efavirenz for improved oral bioavailability: form *Drug Dev. Ind. Pharm.* 40 (2014) 80–91, <https://doi.org/10.3109/03639045.2012.746362>.
- [41] J.S. Negi, P. Chattopadhyay, A.K. Sharma, V. Ram, Development of solid lipid nanoparticles (SLNs) of lopinavir using hot self nano-emulsification (SNE) technique, *Eur. J. Pharmaceut. Sci.* 48 (2013) 231–239, <https://doi.org/10.1016/j.ejps.2012.10.022>.
- [42] Y.R. a Neupane, M. a Srivastava, N. a Ahmad, N. b Kumar, A. b Bhatnagar, \* Kohli, Kanchan a, Lipid based nanocarrier system for the potential oral delivery of decitabine: formulation design, characterization, ex vivo, and in vivo assessment, *Int. J. Pharm.* 477 (2014) 601–612, <https://doi.org/10.1016/j.ijpharm.2014.11.001>.
- [43] S.M.T. Cavalcanti, C. Nunes, S.A. Costa Lima, J.L. Soares-Sobrinho, S. Reis, Optimization of nanostructured lipid carriers for Zidovudine delivery using a microwave-assisted production method, *Eur. J. Pharmaceut. Sci.* 122 (2018) 22–30, <https://doi.org/10.1016/j.ejps.2018.06.017>.
- [44] ICH guideline Q1A(R2), ICH harmonised tripartite guideline, stability testing of new drug substances and products, *Curr. Step 4* (2003) 24, <https://doi.org/10.1136/bmj.333.7574.873-a>.
- [45] P.V. Dangre, S.B. Shinde, S.J. Surana, P.G. Jain, S.S. Chalikwar, Development and exploration on flowability of solid self-nanoemulsifying drug delivery system of morin hydrate, *Adv. Powder Technol.* 33 (2022), 103716, <https://doi.org/10.1016/j.apt.2022.103716>.
- [46] C.V. Pardeshi, P.V. Rajput, V.S. Belgamwar, A.R. Tekade, S.J. Surana, Novel surface modified solid lipid nanoparticles as intranasal carriers for ropinivole hydrochloride: application of factorial design approach, *Drug Deliv.* 20 (2013) 47–56, <https://doi.org/10.3109/10717544.2012.752421>.
- [47] P.V. Dangre, P.P. Dusad, A.D. Singh, S.J. Surana, K.K. Chaturvedi, S.S. Chalikwar, Fabrication of hesperidin self-micro-emulsifying nutraceutical delivery system embedded in sodium alginate beads to elicit gastric stability, *Polym. Bull.* 79 (2022) 605–626, <https://doi.org/10.1007/s00289-020-03507-7>.
- [48] P.S. Hiremath, K.S. Soppimath, G.V. Betageri, Proliposomes of exemestane for improved oral delivery: formulation and in vitro evaluation using PAMPA, Caco-2 and rat intestine, *Int. J. Pharm.* 380 (2009) 96–104, <https://doi.org/10.1016/j.ijpharm.2009.07.008>.
- [49] S. Martins, I. Tho, I. Reimold, G. Fricker, E. Souto, Brain delivery of camptothecin by means of solid lipid nanoparticles: formulation design, in vitro and in vivo studies, *Int. J. Pharm.* 439 (2012) 49–62, <https://doi.org/10.1016/j.ijpharm.2012.09.054>.
- [50] A. Patil-Gadhe, V. Pokharkar, Montelukast-loaded nanostructured lipid carriers: Part I Oral bioavailability improvement, *Eur. J. Pharm. Biopharm.* 88 (2014) 160–168, <https://doi.org/10.1016/j.ejpb.2014.05.019>.
- [51] C. Vora, R. Patadia, K. Mittal, R. Mashru, Risk based approach for design and optimization of site specific delivery of isoniazid, *Int. J. Pharm.* 455 (2013) 169–181, <https://doi.org/10.1007/s40005-014-0170-z>.
- [52] J. Shojaeiarani, D. Bajwa, G. Holt, Sonication amplitude and processing time influence the cellulose nanocrystals morphology and dispersion, *Nanocomposites* 6 (2020) 41–46, <https://doi.org/10.1080/20550324.2019.1710974>.
- [53] S.B. Mahamat Nor, P.M. Woi, S.H. Ng, Characterisation of ionic liquids nanoemulsion loaded with piroxicam for drug delivery system, *J. Mol. Liq.* 234 (2017) 30–39, <https://doi.org/10.1016/j.molliq.2017.03.042>.
- [54] N. Akhtar, M.U. Rehman, H.M.S. Khan, F. Rasool, T. Saeed, Penetration enhancing effect of polysorbate 20 and 80 on the in vitro percutaneous absorption of L-ascorbic, *Acid* 10 (2011) 281–288, <https://doi.org/10.4314/tjpr.v10i3.1>.